

A posteriori error estimates for nonconforming finite element methods for fourth-order problems on rectangles

Carsten Carstensen · Dietmar Gallistl · Jun Hu

Received: 27 February 2012 / Revised: 22 September 2012 / Published online: 26 October 2012
© Springer-Verlag Berlin Heidelberg 2012

Abstract The a posteriori error analysis of conforming finite element discretisations of the biharmonic problem for plates is well established, but nonconforming discretisations are more easy to implement in practice. The a posteriori error analysis for the Morley plate element appears very particular because two edge contributions from an integration by parts vanish simultaneously. This crucial property is lacking for popular rectangular nonconforming finite element schemes like the nonconforming rectangular Morley finite element, the incomplete biquadratic finite element, and the Adini finite element. This paper introduces a novel methodology and utilises some

Dedicated to Professor Z.-C. Shi in honour of his 80th birthday.

This project was supported by the Chinesisch-Deutsches Zentrum project GZ578. The first two authors were partially supported by the DFG Research Center MATHEON. The research of the third author was supported by the NSFC Project 10971005, partially supported by the NSFC Project 11271035 and by the NSFC Key Project 11031006.

C. Carstensen (✉) · D. Gallistl
Institut für Mathematik, Humboldt-Universität zu Berlin, Unter den Linden 6,
10099 Berlin, Germany
e-mail: cc@math.hu-berlin.de

D. Gallistl
e-mail: gallistl@math.hu-berlin.de

C. Carstensen
Department of Computational Science and Engineering, Yonsei University,
120-749 Seoul, Korea

J. Hu (✉)
LMAM and School of Mathematical Sciences, Peking University,
Beijing 100871, Peoples Republic of China
e-mail: hujun@math.pku.edu.cn

conforming discrete space on macro elements to prove reliability and efficiency of an explicit residual-based a posteriori error estimator. An application to the Morley triangular finite element shows the surprising result that *all* averaging techniques yield reliable error bounds. Numerical experiments confirm the reliability and efficiency for the established a posteriori error control on uniform and graded tensor-product meshes.

Mathematics Subject Classification (2000) 65N10 · 65N15 · 35J25

1 Introduction

Computer simulations of plates with conforming finite element methods (FEMs) encounter the difficulty of C^1 continuity and complicated higher-order finite elements. The simplest examples are the Argyris finite element with 21 degrees of freedom or the HCT finite element with 9 or 12 degrees of freedom. One possibility for moderately thin plates is the change of the smooth material model towards a Reissner-Mindlin plate. Since this is problematic for thin plates and impossible for general fourth-order problems, nonconforming plate elements became very popular in computational mechanics. The Morley finite element is perhaps the most prominent nonconforming triangular finite element. Rectangular finite elements are frequently used in practice like the Bogner-Fox-Schmit finite element, the Adini finite element, the rectangular Morley finite element, or the incomplete biquadratic finite element. The a priori error analysis has a long tradition and we refer to [12, 22, 24, 30].

The a posteriori error analysis is rather immediate for conforming plate elements as sketched in [26]. The milestones [2, 3, 19, 20] for the Morley finite element method explore some very particular properties of the ansatz functions. This paper aims at a generalisation of the general unifying a posteriori error analysis [9, 10] for second-order elliptic PDEs to fourth-order problems to cover the aforementioned rectangular nonconforming plate finite element methods. The natural a posteriori error estimator for the nonconforming discrete solution u_{NC} for the right-hand side f on a partition \mathcal{T} reads

$$\begin{aligned} & \sum_{T \in \mathcal{T}} h_T^4 \|f\|_{L^2(T)}^2 + \sum_{E \in \mathcal{E}} h_E \|[D_{\text{NC}}^2 u_{\text{NC}}]_E \tau_E\|_{L^2(E)}^2 \\ & + \sum_{E \in \mathcal{E}(\Omega)} \left(h_E \|[D_{\text{NC}}^2 u_{\text{NC}}]_E \nu_E\|_{L^2(E)}^2 + h_E^3 \|[\text{div}_{\text{NC}} D_{\text{NC}}^2 u_{\text{NC}}]_E \cdot \nu_E\|_{L^2(E)}^2 \right). \quad (1.1) \end{aligned}$$

(Details on the notation of the jumps $[\cdot]_E$ across an edge E with normal ν_E and tangent τ_E of length h_E follow in Sect. 2 below.) This paper establishes some abstract decomposition theorem (see Sect. 3) which substitutes the use of the Helmholtz decomposition for second-order PDEs and proves the a posteriori control by (1.1). The purpose of this paper is to analyse nonconforming rectangular finite elements from [30, 31], namely the rectangular Morley element, the incomplete biquadratic element and the Adini finite element. One difficulty arises from the fact that the discrete spaces cannot contain proper conforming finite element subspaces. Given the discrete solution u_{NC} ,

the following key terms need to be controlled for some test function $v \in H_0^2(\Omega)$,

$$\int_E \left\langle D_{\text{NC}}^2 u_{\text{NC}} \right\rangle_E \nu_E \cdot [\nabla_{\text{NC}}(v - I_{\text{NC}}v)]_E ds, \int_E \left\langle \text{div}_{\text{NC}} D_{\text{NC}}^2 u_{\text{NC}} \right\rangle_E \cdot \nu_E [v - I_{\text{NC}}v]_E ds. \tag{1.2}$$

Here, I_{NC} is some interpolation operator associated to the nonconforming finite element space; D_{NC}^2 and div_{NC} denote the piecewise Hessian and divergence. If the nonconforming finite element space contained the lowest-order conforming finite element space as a subspace, those two terms in (1.2) would vanish. This happens for the nonconforming triangular Morley FEM because $D_{\text{NC}}^2 u_{\text{NC}}$ is piecewise constant and $\int_E [\nabla_{\text{NC}} v]_E ds = 0$ [2, 3, 19, 20, 27]. For the discontinuous Galerkin method, it follows immediately from the definition of the methods that those terms do not arise [6, 14, 17]. For the Ciarlet–Raviart and the Hellan–Herrmann–Johnson method, those terms of (1.2) do not appear [11, 16, 21].

The main result of this paper establishes reliability and efficiency for the rectangular Morley and the incomplete biquadratic FEM while the reliability of the a posteriori error estimator for the Adini finite element method is left open.

The paper is organised as follows. Section 2 provides the basic notation and the definition of the error estimator. Section 3 provides an abstract error decomposition into the equilibrium error and the consistency error. The applications in Sects. 3.2–3.4 generalise the a posteriori error analysis for nonconforming Crouzeix–Raviart and Morley finite elements on triangles and prove that all averaging techniques are reliable. The consistency error will be analysed in Sect. 4 and the equilibrium error will be analysed in Sect. 5.

Throughout the paper, standard notation on Lebesgue and Sobolev spaces is employed. The space of \mathbb{R}^2 -valued H^1 functions with vanishing integral mean over the domain Ω is denoted by $H^1(\Omega; \mathbb{R}^2)/\mathbb{R}^2$. The dot denotes the product of two one-dimensional lists of the same length while the colon denotes the Euclid product of matrices, e.g., $a \cdot b = a^\top b \in \mathbb{R}$ for $a, b \in \mathbb{R}^2$ and $A : B = \sum_{j,k=1}^2 A_{jk} B_{jk}$ for 2×2 matrices A, B . The symmetric part of a matrix A is denoted by $\text{sym}A$. The notation $a \lesssim b$ abbreviates $a \leq Cb$ for a positive generic constant C that may depend on the domain Ω but not on the mesh-size. The notation $a \approx b$ stands for $a \lesssim b \lesssim a$. The measure $|\cdot|$ is context-sensitive and refers to the number of elements of some finite set or the length of an edge or the area of some domain and not just the modulus of a real number or the Euclidean length of a vector.

2 Preliminaries

2.1 Data and basic notation

Let Ω be some bounded Lipschitz domain in \mathbb{R}^2 with polygonal boundary and outer unit normal $\nu = (\nu_1, \nu_2)$ and let \mathcal{T} be some shape-regular triangulation of Ω into rectangles such that $\cup \mathcal{T} = \overline{\Omega}$. Let \mathcal{E} denote the set of edges and let \mathcal{N} denote the set of vertices of \mathcal{T} , while $\mathcal{E}(\Omega)$ denotes the interior edges and $\mathcal{E}(\partial\Omega)$ denotes

the edges on the boundary $\partial\Omega$ of Ω . Analogously, let $\mathcal{N}(\Omega)$ (resp. $\mathcal{N}(\partial\Omega)$) denote the vertices in the interior of Ω (resp. on the boundary of Ω). The edges of a rectangle $T \in \mathcal{T}$ are denoted by $\mathcal{E}(T)$ and the set of vertices of T is denoted by $\mathcal{N}(T)$. The outward-pointing unit normal of T is denoted by ν_T . The midpoint of an edge E is denoted by $\text{mid}(E)$ while $\text{mid}(T)$ denotes the barycentre of T . The piecewise constant function $h_{\mathcal{T}} = \text{diam}(\mathcal{T})$ has the value $h_T := \text{diam}(T)$ for $T \in \mathcal{T}$, while $h_E = |E|$ is the length of an edge E . Given any $z \in \mathcal{N}$, $\mathcal{E}(z)$ denotes the set of edges sharing the vertex z , and $\mathcal{T}(z)$ is the union of the triangles which contain z as a node. Given any $E \in \mathcal{E}$ parallel to the x -axis, the fixed normal vector is $\nu_E := (0, 1)$ and the tangential vector is $\tau_E := (-1, 0)$. For an edge E which is parallel to the y -axis, set $\nu_E := (1, 0)$ and $\tau_E := (0, 1)$. Given any $E \in \mathcal{E}(\Omega)$ with $E = T_+ \cap T_-$ for two neighbouring rectangles (by convention T_+ has the outer unit normal $\nu_{T_+} = \nu_E$), denote the edge-patch of E by $\omega_E := \text{int}(T_+ \cup T_-)$. Given any (possibly vector-valued) function ν , define the jump and the average of ν of across E by

$$[\nu]_E := \nu|_{T_+} - \nu|_{T_-} \quad \text{and} \quad \langle \nu \rangle_E := (\nu|_{T_+} + \nu|_{T_-})/2 \quad \text{along } E.$$

For a boundary edge $E \in \mathcal{E}(\partial\Omega) \cap \mathcal{E}(T_+)$, the partner $\nu|_{T_-}$ is set zero. Given a function $f \in L^2(\Omega)$, the oscillations read

$$\text{osc}^2(f, \mathcal{T}) := \sum_{T \in \mathcal{T}} h_T^4 \|f - f_T\|_{L^2(T)}^2 \quad \text{with } f_T := |T|^{-1} \int_T f \, dx.$$

For a differentiable vector field $\beta = (\beta_1, \beta_2)$, the operators Curl and curl read

$$\text{Curl}\beta := \begin{pmatrix} -\partial\beta_1/\partial x_2 & \partial\beta_1/\partial x_1 \\ -\partial\beta_2/\partial x_2 & \partial\beta_2/\partial x_1 \end{pmatrix} \quad \text{and} \quad \text{curl}\beta := \frac{\partial\beta_2}{\partial x_1} - \frac{\partial\beta_1}{\partial x_2}.$$

For any matrix $\sigma \in \mathbb{R}^{2 \times 2}$, the divergence reads

$$\text{div}\sigma := \begin{pmatrix} \partial\sigma_{11}/\partial x_1 + \partial\sigma_{12}/\partial x_2 \\ \partial\sigma_{21}/\partial x_1 + \partial\sigma_{22}/\partial x_2 \end{pmatrix}.$$

The piecewise action of the differential operators $\nabla, \partial, D^2, \text{div}, \Delta^2, \text{curl}$, reads $\nabla_{\text{NC}}, \partial_{\text{NC}}, D^2_{\text{NC}}, \text{div}_{\text{NC}}, \Delta^2_{\text{NC}}, \text{curl}_{\text{NC}}$.

For $T \in \mathcal{T}$, the spaces of polynomial functions of total or partial degree $k \in \mathbb{N}$ are denoted by

$$P_k(T) := \{v \in L^2(T) \mid v \text{ is a polynomial of total degree } \leq k\},$$

$$Q_k(T) := \{v \in L^2(T) \mid v \text{ is a polynomial of partial degree } \leq k\}.$$

The discrete function spaces read

$$\begin{aligned}
 P_k(\mathcal{T}) &:= \{v \in L^2(\Omega) \mid \forall T \in \mathcal{T}, v|_T \in P_k(T)\}, \\
 P_k(\mathcal{T}; \mathbb{R}_{\text{sym}}^{2 \times 2}) &:= \{v \in L^2(\Omega; \mathbb{R}_{\text{sym}}^{2 \times 2}) \mid \forall j, \ell = 1, 2, v_{j\ell} \in P_k(\mathcal{T})\}, \\
 Q_k(\mathcal{T}) &:= \{v \in L^2(\Omega) \mid \forall T \in \mathcal{T}, v|_T \in Q_k(T)\}, \\
 H^2(\mathcal{T}) &:= \{v \in L^2(\Omega) \mid \forall T \in \mathcal{T}, v|_T \in H^2(T)\}.
 \end{aligned}$$

It is convenient to introduce the local coordinates $-1 \leq \xi, \eta \leq 1$ for a rectangle $T \in \mathcal{T}$ with width $2h_x(T)$ in x -direction and $2h_y(T)$ in y -direction. The midpoint $\text{mid}(T) = (\text{mid}(T, 1), \text{mid}(T, 2))$ defines the coordinate transform

$$\xi|_T(x, y) := \frac{x - \text{mid}(T, 1)}{h_x(T)} \quad \text{and} \quad \eta|_T := \frac{y - \text{mid}(T, 2)}{h_y(T)}.$$

2.2 Kirchhoff plate bending problem

Define the scalar product

$$a(v, w) := \int_{\Omega} D^2 v : D^2 w \, dx \quad \text{for any } v, w \in V := H_0^2(\Omega)$$

with the energy norm $\|\cdot\| := a(\cdot, \cdot)^{1/2}$ on V and the nonconforming bilinear form

$$a_{\text{NC}}(v, w) := \sum_{T \in \mathcal{T}} \int_T D_{\text{NC}}^2 v : D_{\text{NC}}^2 w \, dx \quad \text{for any } v, w \in H^2(\mathcal{T})$$

with the seminorm $\|\cdot\|_{\text{NC}} := a_{\text{NC}}(\cdot, \cdot)^{1/2}$. In its weak formulation, the Kirchhoff plate bending problem reads: Given any $f \in L^2(\Omega)$ seek $u \in V$ such that

$$a(u, v) = \int_{\Omega} f v \, dx \quad \text{for all } v \in V. \tag{2.1}$$

For some nonconforming finite element space $V_{\text{NC}} \subset H^2(\mathcal{T})$ the discrete problem reads: Seek $u_{\text{NC}} \in V_{\text{NC}}$ such that

$$a_{\text{NC}}(u_{\text{NC}}, v_{\text{NC}}) = \int_{\Omega} f v_{\text{NC}} \, dx \quad \text{for all } v_{\text{NC}} \in V_{\text{NC}}. \tag{2.2}$$

All examples in this paper concern discrete spaces such that $(V_{\text{NC}}, a_{\text{NC}})$ is a Hilbert space. In particular, there exists a unique weak solution u of (2.1) respectively a unique discrete solution u_{NC} of (2.2).

2.3 Error estimator

The explicit residual-based a posteriori error estimator has two contributions μ and λ which read, for $T \in \mathcal{T}$,

$$\begin{aligned} \mu^2(T) &:= h_T^4 \|f\|_{L^2(T)}^2 \\ &\quad + \sum_{E \in \mathcal{E}(T) \cap \mathcal{E}(\Omega)} \left(h_E \| [D_{\text{NC}}^2 u_{\text{NC}}]_E \nu_E \|_{L^2(E)}^2 + h_E^3 \| [\text{div}_{\text{NC}} D_{\text{NC}}^2 u_{\text{NC}}]_E \cdot \nu_E \|_{L^2(E)}^2 \right), \\ \lambda^2(T) &:= \sum_{E \in \mathcal{E}(T)} h_E \| [D_{\text{NC}}^2 u_{\text{NC}}]_E \tau_E \|_{L^2(E)}^2. \end{aligned}$$

The main result of this paper in Sects. 4–5 below establishes reliability and efficiency of the explicit residual-based error estimator

$$\mu^2 := \mu^2(\mathcal{T}) := \sum_{T \in \mathcal{T}} \mu^2(T) \quad \text{and} \quad \lambda^2 := \lambda^2(\mathcal{T}) := \sum_{T \in \mathcal{T}} \lambda^2(T)$$

in the sense that

$$\|u - u_{\text{NC}}\|_{\text{NC}}^2 \lesssim \mu^2 + \lambda^2 \lesssim \|u - u_{\text{NC}}\|_{\text{NC}}^2 + \text{osc}^2(f, \mathcal{T}).$$

2.4 Finite element discretisation with rectangles

This paper is devoted to the analysis of three finite element discretisations on rectangles (Fig. 1). A priori error estimates can be found in [12, 22, 24, 30].

The rectangular Morley finite element. Given the shape function space

$$Q_{\text{RM}}(T) = P_2(T) + \text{span}\{x^3, y^3\},$$

the rectangular Morley finite element space [30] is defined by

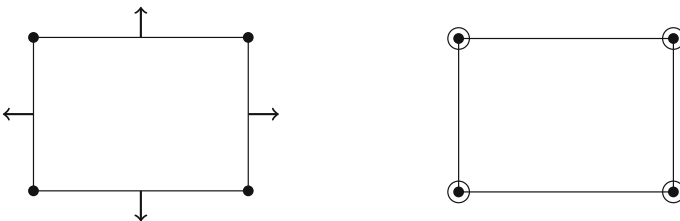


Fig. 1 The degrees of freedom for the rectangular Morley and incomplete biquadratic FEM (left) and for the Adini FEM (right)

$$V_{\text{RM}} = \{v_{\text{RM}} \in Q_{\text{RM}}(\mathcal{T}) \mid v_{\text{RM}} \text{ is continuous at } \mathcal{N}(\Omega) \text{ and vanishes at } \mathcal{N}(\partial\Omega), \\ \nabla_{\text{NC}} v_{\text{RM}} \cdot \nu_E \text{ is continuous at the midpoint of any} \\ E \text{ in } \mathcal{E}(\Omega) \text{ and vanishes for } E \in \mathcal{E}(\partial\Omega)\}.$$

The incomplete biquadratic finite element. The incomplete biquadratic nonconforming finite element was proposed in [31] and analysed in [24]. The shape function space reads

$$Q_{\text{IB}}(T) = P_2(T) + \text{span}\{x^2y, y^2x\}.$$

The incomplete biquadratic finite element space is defined by

$$V_{\text{IB}} = \left\{ v_{\text{IB}} \in Q_{\text{IB}}(\mathcal{T}) \mid v_{\text{IB}} \text{ is continuous at } \mathcal{N}(\Omega) \text{ and vanishes at } \mathcal{N}(\partial\Omega), \\ \nabla_{\text{NC}} v_{\text{IB}} \cdot \nu_E \text{ is continuous at the midpoint of any} \\ E \text{ in } \mathcal{E}(\Omega) \text{ and vanishes for } E \in \mathcal{E}(\partial\Omega) \right\}.$$

The Adini finite element. The shape function space reads

$$Q_{\text{AD}}(T) = P_3(T) + \text{span}\{x^3y, y^3x\}.$$

The Adini finite element space [12,22] is defined by

$$V_{\text{AD}} = \left\{ v_{\text{AD}} \in Q_{\text{AD}}(\mathcal{T}) \mid v_{\text{AD}} \text{ and } \nabla_{\text{NC}} v_{\text{AD}} \text{ are continuous at } \mathcal{N}(\Omega) \\ \text{and vanish at } \mathcal{N}(\partial\Omega) \right\}.$$

3 Error decomposition

This section is devoted to some abstract error decomposition theorem which replaces the Helmholtz decomposition in the standard a posteriori error analysis. Section 3.1 gives an abstract formulation and Sects. 3.2–3.3 discuss two standard applications with novel proofs for possibly multiply connected domains.

3.1 Abstract error decomposition in Hilbert spaces

Let V and V_{NC} denote two linear subspaces of some vector space H so that the sum $V + V_{\text{NC}}$ is a well defined vector space. Suppose that the sum $V + V_{\text{NC}}$ is endowed with some scalar product $\langle \cdot, \cdot \rangle$ and induced norm $\|\cdot\|$. Suppose that $(V, \|\cdot\|)$ is complete with dual space V^* so that, for any $v_{\text{NC}} \in V + V_{\text{NC}}$, there uniquely exists the best approximation $Pv_{\text{NC}} \in V$ in the sense that

$$\text{dist}(v_{\text{NC}}, V) := \min_{w \in V} \|v_{\text{NC}} - w\| = \|v_{\text{NC}} - Pv_{\text{NC}}\|.$$

Theorem 1 (abstract error decomposition) Any $u \in V$ and $u_{\text{NC}} \in V_{\text{NC}}$ with $\text{Res} := \langle u - u_{\text{NC}}, \cdot \rangle \in V^*$ and its dual norm

$$\|\text{Res}\|_{V^*} := \sup_{v \in V \setminus \{0\}} \text{Res}(v) / \|v\|,$$

satisfy

$$\|u - u_{\text{NC}}\|^2 = \|\text{Res}\|_{V^*}^2 + \text{dist}^2(u_{\text{NC}}, V).$$

Proof The best-approximation $Pu_{\text{NC}} \in V$ satisfies $\langle u_{\text{NC}} - Pu_{\text{NC}}, v \rangle = 0$ for all v in V . For $v := u - Pu_{\text{NC}}$, the Pythagoras theorem and the Riesz isomorphism imply

$$\|u - u_{\text{NC}}\|^2 = \|u - Pu_{\text{NC}}\|^2 + \text{dist}^2(u_{\text{NC}}, V) = \|\text{Res}\|_{V^*}^2 + \text{dist}^2(u_{\text{NC}}, V).$$

□

3.2 Crouzeix–Raviart NCFEM for Poisson model problem

The Crouzeix–Raviart nonconforming finite element space (Fig. 2)

$$\text{CR}_0^1(\mathcal{T}) := \{v_{\text{CR}} \in P_1(\mathcal{T}) \mid v_{\text{CR}} \text{ is continuous at mid}(\mathcal{E}(\Omega)) \text{ and vanishes at mid}(\mathcal{E}(\partial\Omega))\}$$

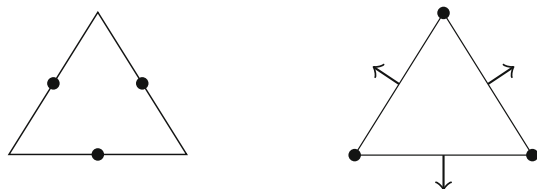
is endowed with the discrete scalar product

$$a_{\text{NC}}(v, w) := \int_{\Omega} \nabla_{\text{NC}} v \cdot \nabla_{\text{NC}} w \, dx \quad \text{for any } v, w \in H_0^1(\Omega) + \text{CR}_0^1(\mathcal{T}).$$

The discrete problem seeks $u_{\text{NC}} \in \text{CR}_0^1(\mathcal{T})$ such that

$$a_{\text{NC}}(u_{\text{NC}}, v_{\text{NC}}) = \int_{\Omega} f v_{\text{NC}} \, dx \quad \text{for all } v_{\text{NC}} \in \text{CR}_0^1(\mathcal{T}).$$

Fig. 2 The Crouzeix–Raviart (left) and the Morley (right) nonconforming finite element



The nonconforming interpolation operator $I_{\text{NC}} : H_0^1(\Omega) \rightarrow \text{CR}_0^1(\mathcal{T})$ is defined via

$$\int_E I_{\text{NC}} v \, ds = \int_E v \, ds \quad \text{for all } E \in \mathcal{E}$$

and so

$$\nabla_{\text{NC}} I_{\text{NC}} v = |T|^{-1} \int_T \nabla v \, dx \quad \text{for any } T \in \mathcal{T}.$$

Since $\nabla_{\text{NC}} u_{\text{NC}}$ is piecewise constant, this implies

$$a_{\text{NC}}(u_{\text{NC}}, v) = a_{\text{NC}}(u_{\text{NC}}, I_{\text{NC}} v) = \int_{\Omega} f I_{\text{NC}} v \, dx.$$

Hence,

$$\begin{aligned} \text{Res}(v) &= \int_{\Omega} f(v - I_{\text{NC}} v) \, dx \leq \|h_{\mathcal{T}} f\|_{L^2(\Omega)} \|h_{\mathcal{T}}^{-1}(v - I_{\text{NC}} v)\|_{L^2(\Omega)} \\ &\leq C_{\text{apx}} \|h_{\mathcal{T}} f\|_{L^2(\Omega)} \|v\|. \end{aligned}$$

This direct argument seems to be new and leads to some explicit stability constant C_{apx} from [8].

It is emphasised that this novel proof applies to multiply connected domains while in this case the alternative usage of the Helmholtz decomposition is not immediate.

3.3 Triangular Morley finite element

For a regular triangulation \mathcal{T} into triangles, the Morley finite element space [23] reads

$$\begin{aligned} M(\mathcal{T}) := \left\{ v_{\text{M}} \in P_2(\mathcal{T}) \mid v_{\text{M}} \text{ is continuous at } \mathcal{N}(\Omega), \text{ and vanishes at } \mathcal{N}(\partial\Omega), \right. \\ \left. \forall E \in \mathcal{E}(\Omega), \int_E \left[\frac{\partial v_{\text{M}}}{\partial \nu_E} \right] ds = 0, \forall E \in \mathcal{E}(\partial\Omega), \int_E \frac{\partial v_{\text{M}}}{\partial \nu_E} ds = 0 \right\}. \end{aligned}$$

Let u_{M} be the solution of the discrete problem (2.2) with the triangular Morley finite element method. Let I_{M} denote the canonical interpolation operator for the Morley finite element method, which is defined, for any $v \in V = H_0^2(\Omega)$, by

$$\begin{aligned} I_{\text{M}} v(z) &= v(z) && \text{for any } z \in \mathcal{N}, \\ \int_E \nabla_{\text{NC}} I_{\text{M}} v \, ds &= \int_E \nabla v \, ds && \text{for any } E \in \mathcal{E}. \end{aligned}$$

The mean-value property of the interpolation operator I_M for the piecewise Hessian and the stability of the interpolation operator [12] prove for any $v \in V$ with $\|v\| = 1$

$$\begin{aligned} a_{\text{NC}}(u - u_M, v) &= \int_{\Omega} D^2u : D^2v \, dx - \int_{\Omega} D_{\text{NC}}^2 u_M : D_{\text{NC}}^2 I_M v \, dx \\ &= \int_{\Omega} f(v - I_M v) \, dx \lesssim \|h_{\mathcal{T}}^2 f\|_{L^2(\Omega)} \end{aligned}$$

and so

$$\|\text{Res}\|_{V^*} \lesssim \|h_{\mathcal{T}}^2 f\|_{L^2(\Omega)}.$$

The proof applies to multiply connected domains and so generalises [2, 19].

3.4 Averaging estimator for Morley FEM

A restriction to simply connected domains allows for reliability of any averaging estimators in the context of [1].

Theorem 2 *Let Ω be simply connected and let u_M be the solution of the discrete problem (2.2) with the triangular Morley finite element method. Then any $\sigma \in P_k(\mathcal{T}; \mathbb{R}_{\text{sym}}^{2 \times 2})$ satisfies*

$$\|u - u_M\|_{\text{NC}} \lesssim \|h_{\mathcal{T}}^2 f\|_{L^2(\Omega)} + \|\sigma - D_{\text{NC}}^2 u_M\|_{L^2(\Omega)} + \left(\sum_{E \in \mathcal{E}} h_E \|\llbracket \sigma \rrbracket_E \tau_E\|_{L^2(E)}^2 \right)^{1/2}.$$

Proof Given $\sigma \in P_k(\mathcal{T}; \mathbb{R}_{\text{sym}}^{2 \times 2})$ with a Helmholtz decomposition of [2, Lemma 1] for a simply connected domain, there exist $\psi \in H_0^2(\Omega)$ and $\phi \in H^1(\Omega; \mathbb{R}^2)/\mathbb{R}^2$ such that

$$\sigma = D^2\psi + \text{symCurl}\phi$$

with the stability property $\|\text{Curl}\phi\|_{L^2(\Omega)} \lesssim \|\text{symCurl}\phi\|_{L^2(\Omega)}$. Then, in generalisation of [7, Theorem 2.2],

$$\min_{v \in V} \|\sigma - D^2v\|_{L^2(\Omega)} \lesssim \sup_{\substack{\varphi \in H^1(\Omega; \mathbb{R}^2)/\mathbb{R}^2 \\ \|\nabla\varphi\|_{L^2(\Omega)}=1}} \int_{\Omega} \sigma : \text{Curl}\varphi \, dx.$$

Let $\varphi_C \in P_1(\mathcal{T}) \cap C(\bar{\Omega})$ denote the Clément quasi-interpolant [13] of $\varphi \in H^1(\Omega)$ with $\|\nabla\varphi\|_{L^2(\Omega)} = 1$. Since $v_E \cdot \text{Curl}\varphi_C = \partial\varphi_C/\partial s$ is continuous along any edge $E \in \mathcal{E}$,

$$\int_{\Omega} D_{\text{NC}}^2 u_M : \text{Curl} \varphi_C \, dx = \sum_{E \in \mathcal{E}} \int_E [\nabla_{\text{NC}} u_M]_E \cdot \text{Curl} \varphi_C \nu_E \, ds = 0.$$

Therefore,

$$\int_{\Omega} \sigma : \text{Curl} \varphi \, dx = \int_{\Omega} \sigma : \text{Curl}(\varphi - \varphi_C) \, dx + \int_{\Omega} (\sigma - D_{\text{NC}}^2 u_M) : \text{Curl} \varphi_C \, dx. \tag{3.1}$$

An integration by parts, followed by inverse and trace estimates and the approximation and stability property of the quasi-interpolation operator prove

$$\begin{aligned} & \int_{\Omega} \sigma : \text{Curl}(\varphi - \varphi_C) \, dx \\ &= - \int_{\Omega} \text{curl}_{\text{NC}}(\sigma - D_{\text{NC}}^2 u_M) \cdot (\varphi - \varphi_C) \, dx + \sum_{E \in \mathcal{E}} \int_E [\sigma]_E \tau_E \cdot (\varphi - \varphi_C) \, ds \\ &\lesssim \sum_{T \in \mathcal{T}} h_T^{-1} \|\sigma - D_{\text{NC}}^2 u_M\|_{L^2(\Omega)} \, h_T \|D\varphi\|_{L^2(\omega_T)} \\ &\quad + \sum_{E \in \mathcal{E}} \|[\sigma]_E \tau_E\|_{L^2(\Omega)} h_E^{1/2} \|D\varphi_C\|_{L^2(\omega_E)} \\ &\lesssim \|\sigma - D_{\text{NC}}^2 u_M\|_{L^2(\Omega)} + \left(\sum_{E \in \mathcal{E}} h_E \|[\sigma]_E \tau_E\|_{L^2(E)}^2 \right)^{1/2}. \end{aligned}$$

This and a triangle inequality conclude the proof: Indeed,

$$\begin{aligned} \min_{v \in V} \|D_{\text{NC}}^2 u_M - D^2 v\|_{L^2(\Omega)} &\leq \|\sigma - D_{\text{NC}}^2 u_M\|_{L^2(\Omega)} + \min_{v \in V} \|\sigma - D^2 v\|_{L^2(\Omega)} \\ &\lesssim \|\sigma - D_{\text{NC}}^2 u_M\|_{L^2(\Omega)} + \left(\sum_{E \in \mathcal{E}} h_E \|[\sigma]_E \tau_E\|_{L^2(E)}^2 \right)^{1/2}. \end{aligned}$$

□

The particular choice $\sigma = D_{\text{NC}}^2 u_M$ verifies the reliability of the estimator from [19]. For the two-dimensional case, inverse and Poincaré inequalities prove the equivalence of this estimator to the estimator from [2]. To obtain the reliability of *any* averaging of the piecewise Hessian, define the space $\Sigma := P_k(\mathcal{T}; \mathbb{R}_{\text{sym}}^{2 \times 2}) \cap C(\Omega; \mathbb{R}_{\text{sym}}^{2 \times 2})$. It holds

$$\text{dist}(u_M, V) \lesssim \min_{\sigma \in \Sigma} \left(\|\sigma - D_{\text{NC}}^2 u_M\|_{L^2(\Omega)} + \left(\sum_{E \in \mathcal{E}(\partial\Omega)} h_E \|[\sigma]_E \tau_E\|_{L^2(E)}^2 \right)^{1/2} \right).$$

4 Analysis of the consistency error

This section establishes a general a posteriori control of the consistency error for finite element functions u_{NC} which are continuous at $\mathcal{N}(\Omega)$ and satisfy the weak continuity condition

$$\forall E \in \mathcal{E} \quad \exists x \in E \quad \left[\frac{\partial u_{\text{NC}}}{\partial \nu_E}(x) \right]_E = 0. \tag{4.1}$$

In particular, this includes the rectangular Morley FEM, the incomplete biquadratic FEM, and the Adini FEM.

Theorem 3 *Let $u_{\text{NC}} \in Q_3(\mathcal{T})$ be continuous at \mathcal{N} and vanish at $\mathcal{N}(\partial\Omega)$. Let u_{NC} satisfy the weak continuity condition (4.1) and recall the definition of $\lambda(\mathcal{T})$ from Sect. 2.3. Then*

$$\text{dist}(u_{\text{NC}}, V) \approx \lambda(\mathcal{T}).$$

Proof of reliability: the analysis of the consistency error employs the Bogner-Fox-Schmit Q_3 finite element space [12]

$$V_{\text{BFS}} = \{v_C \in C^1(\Omega) \cap Q_3(\mathcal{T}) \mid v_C|_{\partial\Omega} = \partial v_C / \partial \nu|_{\partial\Omega} = 0\}.$$

The finite element functions are determined by their values, first-order derivatives, and the mixed second-order derivative at the vertices (see Fig. 3).

The averaging operator [4] $\mathcal{A} : V_{\text{NC}} \rightarrow V_{\text{BFS}}$ is defined, for all $z \in \mathcal{N}(\Omega)$ by

$$\begin{aligned} (\mathcal{A}v_{\text{NC}})(z) &= \frac{1}{|\mathcal{T}(z)|} \sum_{T \in \mathcal{T}(z)} (v_{\text{NC}}|_T)(z), \\ (\nabla \mathcal{A}v_{\text{NC}})(z) &= \frac{1}{|\mathcal{T}(z)|} \sum_{T \in \mathcal{T}(z)} (\nabla v_{\text{NC}}|_T)(z), \\ \left(\frac{\partial^2 \mathcal{A}v_{\text{NC}}}{\partial x \partial y} \right)(z) &= \frac{1}{|\mathcal{T}(z)|} \sum_{T \in \mathcal{T}(z)} \left(\frac{\partial^2 v_{\text{NC}}|_T}{\partial x \partial y} \right)(z). \end{aligned}$$



Fig. 3 The $C^1 - Q_2$ macro element and the BFS Q_3 finite element

The distance can be estimated by the discrete conforming approximation,

$$\text{dist}^2(u_{\text{NC}}, V) \leq \|D_{\text{NC}}^2(u_{\text{NC}} - \mathcal{A}u_{\text{NC}})\|_{L^2(\Omega)}^2.$$

Let $\varphi_z, \psi_z, \chi_z$ denote the nodal basis function of V_{BFS} at some node $z \in \mathcal{N}$ which satisfy

$$\partial\varphi_z/\partial x = 1, \quad \partial\psi_z/\partial y = 1, \quad \partial^2\chi_z/\partial x\partial y = 1 \quad \text{at } z \in \mathcal{N}$$

and vanish for the remaining degrees of freedom. Since the function u_{NC} is continuous at the vertices, the difference of the nodal values drops out. Hence,

$$\begin{aligned} & \|D_{\text{NC}}^2(u_{\text{NC}} - \mathcal{A}u_{\text{NC}})\|_{L^2(\Omega)}^2 \\ &= \sum_{T \in \mathcal{T}} \left\| \sum_{z \in \mathcal{N}(T)} \partial(u_{\text{NC}}|_T - \mathcal{A}u_{\text{NC}})/\partial x D^2\varphi_z + \partial(u_{\text{NC}}|_T - \mathcal{A}u_{\text{NC}})/\partial y D^2\psi_z \right. \\ & \quad \left. + \partial^2(u_{\text{NC}}|_T - \mathcal{A}u_{\text{NC}})/\partial x\partial y D^2\chi_z \right\|_{L^2(T)}^2. \end{aligned}$$

Some transformation to the reference domain $(-1, 1)^2$ leads to the scaling

$$\|D^2\varphi_z\|_{L^2(T)} \lesssim 1, \quad \|D^2\psi_z\|_{L^2(T)} \lesssim 1, \quad \|D^2\chi_z\|_{L^2(T)} \lesssim h_T$$

(here one requires shape regularity). This proves

$$\begin{aligned} & \text{dist}^2(u_{\text{NC}}, V) \\ & \lesssim \sum_{T \in \mathcal{T}} \sum_{z \in \mathcal{N}(T)} \left(|\nabla(u_{\text{NC}}|_T - \mathcal{A}u_{\text{NC}})(z)|^2 + h_T^2 \left| \frac{\partial^2}{\partial x\partial y}(u_{\text{NC}}|_T - \mathcal{A}u_{\text{NC}})(z) \right|^2 \right). \end{aligned}$$

For any node $z \in \mathcal{N}(T) \cap \mathcal{N}(\Omega)$ which does not belong to $\partial\Omega$, the triangle inequality reveals

$$\begin{aligned} |\nabla(u_{\text{NC}}|_T - \mathcal{A}u_{\text{NC}})(z)| & \leq \sum_{K \in \mathcal{F}(z)} 1/4 |\nabla(u_{\text{NC}}|_T - u_{\text{NC}}|_K)(z)| \\ & \lesssim \sum_{E \in \mathcal{E}(z)} [\nabla_{\text{NC}}u_{\text{NC}}(z)]_E. \end{aligned}$$

A similar argument for the second term and for nodes $z \in \mathcal{N}(\partial\Omega)$ on the boundary proves

$$\text{dist}^2(u_{\text{NC}}, V) \lesssim \sum_{z \in \mathcal{N}} \sum_{E \in \mathcal{E}(z)} \left([\nabla_{\text{NC}}u_{\text{NC}}(z)]_E^2 + h_E^2 \left[\frac{\partial_{\text{NC}}^2}{\partial x\partial y} u_{\text{NC}}(z) \right]_E^2 \right).$$

It follows from an equivalence of norms argument in $P_3(E)$ along an edge $E \in \mathcal{E}$ and Poincaré–Friedrichs inequalities due to the weak continuity condition (4.1) that

$$\begin{aligned}
 |[\nabla_{\text{NC}} u_{\text{NC}}]_E(z)| &\lesssim h_E^{-1/2} \|[\nabla_{\text{NC}} u_{\text{NC}}]_E\|_{L^2(E)} \lesssim h_E^{1/2} \|[D_{\text{NC}}^2 u_{\text{NC}}]_E \tau_E\|_{L^2(E)}, \\
 \left| \left[\frac{\partial_{\text{NC}}^2 u_{\text{NC}}}{\partial x \partial y} \right]_E(z) \right| &\lesssim h_E^{-1/2} \left\| \left[\frac{\partial_{\text{NC}}^2 u_{\text{NC}}}{\partial x \partial y} \right]_E \right\|_{L^2(E)} \lesssim h_E^{-1/2} \|[D_{\text{NC}}^2 u_{\text{NC}}]_E \tau_E\|_{L^2(E)}.
 \end{aligned}
 \tag{4.2}$$

The combination of the previous estimates completes the proof. □

Proof of efficiency: the proof is based on the discrete function technology due to Verfürth [26]. For all $E \in \mathcal{E}$ let $b_E \in H_0^1(\omega_E)$ be the bubble functions with the properties

$$\|b_E\|_{L^\infty(\Omega)} \approx 1 \quad \text{and} \quad \int_E b_E \, ds = |E|.$$

For any $E \in \mathcal{E}$ define $\psi_E := b_E [D_{\text{NC}}^2 u_{\text{NC}}]_E \tau_E$ on E and extend it to $H_0^1(\omega_E)$ as in [26]. Some equivalence of norms plus an integration by parts followed by an inverse estimate argument reveal

$$\begin{aligned}
 \|[D_{\text{NC}}^2 u_{\text{NC}}] \tau_E\|_{L^2(E)}^2 &\approx \int_E [D_{\text{NC}}^2 u_{\text{NC}}] \tau_E \cdot \psi_E \, ds \\
 &= \int_{\omega_E} D_{\text{NC}}^2(u_{\text{NC}} - u) : \text{Curl} \psi_E \, dx \\
 &\leq \|D_{\text{NC}}^2(u - u_{\text{NC}})\|_{L^2(\omega_E)} \|\text{Curl} \psi_E\|_{L^2(\Omega)} \\
 &\lesssim h_E^{-1} \|D_{\text{NC}}^2(u - u_{\text{NC}})\|_{L^2(\omega_E)}^2.
 \end{aligned}$$

□

5 Equilibrium

This section will establish the reliability of the a posteriori error estimator for the rectangular Morley FEM and the incomplete biquadratic FEM. The proof of efficiency is based on the discrete test functions, similar to Sect. 4. The details in the efficiency proof for the equilibrium error are the same as for conforming finite element methods and can be found in [26, Sect. 3.7].

5.1 Reliability for the rectangular Morley FEM

Theorem 4 *The rectangular Morley finite element solution u_{RM} of (2.2) satisfies*

$$\|\text{Res}\|_{V^*}^2 \lesssim \|h_{\mathcal{T}}^2 f\|_{L^2(\Omega)}^2 + \sum_{E \in \mathcal{E}(\Omega)} h_E^3 \|[\text{div}_{\text{NC}} D_{\text{NC}}^2 u_{\text{RM}}] \cdot \nu_E\|_{L^2(E)}^2 \lesssim \mu^2.$$

Proof Let $I_{RM} : V \rightarrow V_{RM}$ denote the interpolation operator defined, for a function $v \in V$, by

$$(I_{RM}v)(z) = v(z) \text{ at any vertex } z \in \mathcal{N},$$

$$\int_E \nabla_{NC} I_{RM}v \cdot \nu_E ds = \int_E \nabla v \cdot \nu_E ds \text{ for any edge } E \in \mathcal{E}.$$

The well-established interpolation theory [5, 25, 30] proves the subsequent approximation and stability property of I_{RM} , for any $T \in \mathcal{T}$,

$$h_T^{-2} \|v - I_{RM}v\|_{L^2(T)} + h_T^{-1} \|\nabla_{NC}(v - I_{RM}v)\|_{L^2(T)} + \|D_{NC}^2(v - I_{RM}v)\|_{L^2(T)} \lesssim \|D^2v\|_{L^2(T)}. \tag{5.1}$$

The discrete problem (2.2) implies, for any $v \in V$ with $\|v\| = 1$, that

$$\text{Res}(v) = \int_{\Omega} f(v - I_{RM}v) dx - a_{NC}(u_{RM}, v - I_{RM}v).$$

Since (5.1), the first term can be controlled as

$$\int_{\Omega} f(v - I_{RM}v) dx \lesssim \|h_{\mathcal{T}}^2 f\|_{L^2(\Omega)}.$$

Two integrations by parts on the rectangle $T \in \mathcal{T}$ and the fact that $\Delta_{NC}^2 u_{RM} = 0$ lead to

$$\begin{aligned} & \int_T D_{NC}^2 u_{RM} : D_{NC}^2(v - I_{RM}v) dx \\ &= \int_{\partial T} (D_{NC}^2 u_{RM} \nu_T) \cdot \nabla_{NC}(v - I_{RM}v) ds \\ & \quad - \int_{\partial T} (v - I_{RM}v)(\text{div}_{NC} D_{NC}^2 u_{RM}) \cdot \nu_T ds. \end{aligned}$$

The definition of the interpolation operator I_{RM} implies

$$\int_E \nabla_{NC}(v - I_{RM}v) ds = 0.$$

Since $D_{NC}^2 u_{RM} \nu_T$ is constant along each edge, it follows

$$\int_{\partial T} (D_{NC}^2 u_{RM} \nu_T) \cdot \nabla_{NC}(v - I_{RM}v) ds = 0.$$

This allows for the following calculations

$$\begin{aligned}
 a_{\text{NC}}(u_{\text{RM}}, v - I_{\text{RM}}v) &= - \sum_{E \in \mathcal{E}(\Omega)} \int_E \left[\text{div}_{\text{NC}} D_{\text{NC}}^2 u_{\text{RM}} \right]_E \cdot \nu_E \langle v - I_{\text{RM}}v \rangle_E ds \\
 &\quad - \sum_{E \in \mathcal{E}(\Omega)} \int_E \left\langle \text{div}_{\text{NC}} D_{\text{NC}}^2 u_{\text{RM}} \right\rangle_E \cdot \nu_E [v - I_{\text{RM}}v]_E ds \\
 &\quad - \sum_{E \in \mathcal{E}(\partial\Omega)} \int_E \text{div}_{\text{NC}} D_{\text{NC}}^2 u_{\text{RM}} \cdot \nu (v - I_{\text{RM}}v) ds.
 \end{aligned}$$

Let I_{Q_1} be the canonical bilinear interpolation operator [5, p.85]. Since $I_{\text{RM}}v$ is continuous at any node $z \in \mathcal{N}$, the elementwise bilinear interpolation leads to a globally continuous function $I_{Q_1} I_{\text{RM}}v$. The continuity and some summation by parts yield

$$\begin{aligned}
 &\sum_{E \in \mathcal{E}(\Omega)} \int_E \left\langle \text{div}_{\text{NC}} D_{\text{NC}}^2 u_{\text{RM}} \right\rangle_E \cdot \nu_E [v - I_{\text{RM}}v]_E ds \\
 &\quad + \sum_{E \in \mathcal{E}(\partial\Omega)} \int_E \text{div}_{\text{NC}} D_{\text{NC}}^2 u_{\text{RM}} \cdot \nu (v - I_{\text{RM}}v) ds \\
 &= \sum_{E \in \mathcal{E}(\Omega)} \int_E \left\langle \text{div}_{\text{NC}} D_{\text{NC}}^2 u_{\text{RM}} \right\rangle_E \cdot \nu_E [I_{Q_1} I_{\text{RM}}v - I_{\text{RM}}v]_E ds \\
 &\quad + \sum_{E \in \mathcal{E}(\partial\Omega)} \int_E \text{div}_{\text{NC}} D_{\text{NC}}^2 u_{\text{RM}} \cdot \nu (I_{Q_1} I_{\text{RM}}v - I_{\text{RM}}v) ds \\
 &= - \sum_{E \in \mathcal{E}(\Omega)} \int_E \left[\text{div}_{\text{NC}} D_{\text{NC}}^2 u_{\text{RM}} \right]_E \cdot \nu_E \langle I_{Q_1} I_{\text{RM}}v - I_{\text{RM}}v \rangle_E ds \\
 &\quad + \sum_{T \in \mathcal{T}} \int_{\partial T} \text{div}_{\text{NC}} D_{\text{NC}}^2 u_{\text{RM}} \cdot \nu_T (I_{Q_1} I_{\text{RM}}v - I_{\text{RM}}v) ds.
 \end{aligned}$$

The interpolation operator I_{Q_1} acts on the shape functions of V_{RM} in terms of the natural coordinates $-1 \leq \xi, \eta \leq 1$ as follows

$$I_{Q_1} \xi^2 = I_{Q_1} \eta^2 = 1, \quad I_{Q_1} \xi^3 = \xi, \quad I_{Q_1} \eta^3 = \eta.$$

Therefore, for any $T \in \mathcal{T}$, there exist constants a_T, b_T, c_T, d_T such that the difference $I_{Q_1} I_{\text{RM}}v - I_{\text{RM}}v$ reads

$$I_{Q_1} I_{\text{RM}}v - I_{\text{RM}}v = a_T(\xi^2 - 1) + b_T(\eta^2 - 1) + c_T(\xi^3 - \xi) + d_T(\eta^3 - \eta).$$

Let E_1, E_3 be the edges parallel to the y -axis. Since $\operatorname{div}_{\text{NC}} D_{\text{NC}}^2 u_{\text{RM}}$ is constant on T and since $(\xi^3 - \xi)|_{E_1} = 0 = (\xi^3 - \xi)|_{E_3}$, it follows

$$\begin{aligned} & \int_{E_1} (I_{Q_1} I_{\text{RM}} v - I_{\text{RM}} v) \operatorname{div}_{\text{NC}} D_{\text{NC}}^2 u_{\text{RM}} \cdot \nu_T \, ds \\ &= - \int_{E_3} (I_{Q_1} I_{\text{RM}} v - I_{\text{RM}} v) \operatorname{div}_{\text{NC}} D_{\text{NC}}^2 u_{\text{RM}} \cdot \nu_T \, ds. \end{aligned}$$

This and analogous arguments for the edges parallel to the x -axis, lead to

$$\sum_{T \in \mathcal{T}} \int_{\partial T} \operatorname{div}_{\text{NC}} D_{\text{NC}}^2 u_{\text{RM}} \cdot \nu_T (I_{Q_1} I_{\text{RM}} v - I_{\text{RM}} v) \, ds = 0.$$

The combination of the previous identities results in

$$a_{\text{NC}}(u_{\text{RM}}, v - I_{\text{RM}} v) = \sum_{E \in \mathcal{E}(\Omega)} \int_E \left[\operatorname{div}_{\text{NC}} D_{\text{NC}}^2 u_{\text{RM}} \right]_E \cdot \nu_E \langle I_{Q_1} I_{\text{RM}} v - v \rangle \, ds.$$

The Cauchy and trace inequalities and the approximation and stability properties of the operators I_{Q_1} and I_{RM} prove

$$a_{\text{NC}}(u_{\text{RM}}, v - I_{\text{RM}} v) \lesssim \sqrt{\sum_{E \in \mathcal{E}(\Omega)} h_E^3 \|\left[\operatorname{div}_{\text{NC}} D_{\text{NC}}^2 u_{\text{RM}} \right]_E \cdot \nu_E\|_{L^2(E)}^2}.$$

5.2 Reliability for the incomplete biquadratic FEM

Theorem 5 *Given a mesh \mathcal{T} generated by red-refinement of a shape regular partition \mathcal{F} of Ω into rectangles, the incomplete biquadratic finite element solution u_{IB} satisfies*

$$\|\operatorname{Res}\|_{V^*} \lesssim \mu.$$

The main ingredient in the proof of reliability is the conforming $C_1 - Q_2$ macro element space from [18]. To this end, let \mathcal{F} be a shape regular partition of Ω into rectangles and divide each rectangle in \mathcal{F} by the red-refinement into four congruent sub-rectangles (Fig. 4) to form the mesh $\mathcal{T} = \text{red}(\mathcal{F})$. The macro $C^1 - Q_2$ finite element space is defined by

$$V_{Q_2} = H_0^2(\Omega) \cap Q_2(\mathcal{T}).$$

Lemma 1 *It holds*

$$\|\operatorname{Res}\|_{V^*} \lesssim \mu + \|\operatorname{Res}\|_{V_{Q_2}^*}.$$

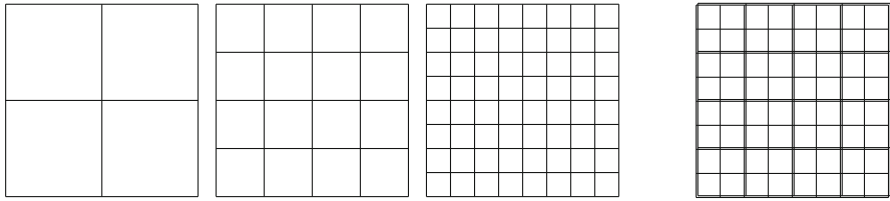


Fig. 4 Three levels of nestedly refined grids, and a macro-element grid

Proof Let $J_{Q_2} : H_0^2(\Omega) \rightarrow V_{Q_2}$ be the quasi-interpolation operator from [18] with the properties $J_{Q_2} v_C = v_C$ for any $v_C \in V_{Q_2}$, and, for any $v \in H_0^2(\Omega)$ with $\|v\| = 1$,

$$h_T^{-2} \|v - J_{Q_2} v\|_{L^2(T)} + h_T^{-1} \|\nabla(v - J_{Q_2} v)\|_{L^2(T)} + \|D_{\text{NC}}^2(v - J_{Q_2} v)\|_{L^2(T)} \lesssim \|D_{\text{NC}}^2 v\|_{L^2(\omega_T)}.$$

The proof of the lemma is based on the split

$$\text{Res}(v) = a_{\text{NC}}(u_{\text{NC}}, v - J_{Q_2} v) - \int_{\Omega} f(v - J_{Q_2} v) \, dx + a_{\text{NC}}(u_{\text{NC}}, J_{Q_2} v) - \int_{\Omega} f J_{Q_2} v \, dx.$$

Two integrations by parts (followed by the Cauchy and trace inequalities) and the approximation and stability properties of the operator J_{Q_2} reveal

$$\begin{aligned} & a_{\text{NC}}(u_{\text{NC}}, v - J_{Q_2} v) - \int_{\Omega} f(v - J_{Q_2} v) \, dx \\ &= \sum_{E \in \mathcal{E}(\Omega)} \left(\int_E [D_{\text{NC}}^2 u_{\text{IB}}]_E \cdot \nu_E \cdot \nabla(v - J_{Q_2} v) \, ds - \int_E [\text{div}_{\text{NC}} D_{\text{NC}}^2 u_{\text{IB}}]_E \cdot \nu_E (v - J_{Q_2} v) \, ds \right) \\ & \quad - \int_{\Omega} f(v - J_{Q_2} v) \, dx \lesssim \mu. \end{aligned}$$

The stability of J_{Q_2} implies

$$\left| a_{\text{NC}}(u_{\text{NC}}, J_{Q_2} v) - \int_{\Omega} f J_{Q_2} v \, dx \right| \lesssim \|\text{Res}\|_{V_{Q_2}^*} \|J_{Q_2} v\| \lesssim \|\text{Res}\|_{V_{Q_2}^*}.$$

The combination of the aforementioned estimates concludes the proof. □

Proof of Theorem 5 Let $u_{\text{IB}} \in V_{\text{IB}}$ denote the solution of (2.2) for the incomplete biquadratic finite element method and let I_{IB} denote the canonical interpolation operator [24] defined, for $v_C \in V_{Q_2}$, by

$$\begin{aligned} (I_{\text{IB}} v_C)(z) &= v_C(z) \text{ for any vertex } z \in \mathcal{N} \\ (\nabla_{\text{NC}} I_{\text{IB}} v_C \cdot \nu_E)(\text{mid}(E)) &= (\nabla v_C \cdot \nu_E)(\text{mid}(E)) \text{ for any edge } E \in \mathcal{E}. \end{aligned} \tag{5.2}$$

The approximation and stability properties from [24] read

$$\begin{aligned}
 & h_T^{-2} \|v_C - I_{IB} v_C\|_{L^2(T)} + h_T^{-1} \|\nabla_{NC}(v_C - I_{IB} v_C)\|_{L^2(T)} \\
 & + \|D_{NC}^2(v_C - I_{IB} v_C)\|_{L^2(T)} \lesssim \|D^2 v_C\|_{L^2(T)}.
 \end{aligned}
 \tag{5.3}$$

The discrete problem (2.2) implies, for any $v_C \in V_{Q_2}$ with $\|v_C\| = 1$, that

$$\text{Res}(v_C) = a_{NC}(u_{IB}, v_C - I_{IB} v_C) - \int_{\Omega} f(v_C - I_{IB} v_C) dx.$$

The second term is bounded with (5.3) by

$$\int_{\Omega} f(v_C - I_{IB} v_C) dx \lesssim \|h_{\mathcal{T}}^2 f\|_{L^2(\Omega)}.$$

Hence, it suffices to prove the estimate

$$a_{NC}(u_{IB}, v_C - I_{IB} v_C) \lesssim \mu.$$

Since I_{IB} is exact for all shape functions of V_{Q_2} except $\xi^2 \eta^2$ (written in natural coordinates), there exists, for any $T \in \mathcal{T}$, some constant c_T such that

$$v_C - I_{IB} v_C|_T = c_T (\xi^2 \eta^2 - 1) \quad \text{in } T \in \mathcal{T}.
 \tag{5.4}$$

An integration by parts reveals

$$\begin{aligned}
 & \int_T D^2 u_{IB} : D^2(v_C - I_{IB} v_C) dx \\
 & = \int_{\partial T} D^2 u_{IB} \nu_T \cdot \nabla(v_C - I_{IB} v_C) ds - \int_T \text{div} D^2 u_{IB} \cdot \nabla(v_C - I_{IB} v_C) dx.
 \end{aligned}$$

Since $\text{div}_{NC} D_{NC}^2 u_{IB}$ is constant on T , and since $\nabla_{NC}(v_C - I_{IB} v_C)$ by (5.4) is an odd function, the volume term vanishes.

Let E_1, E_3 denote the edges of T parallel to the y -axis with $\nu_T|_{E_3} = (1, 0) = -\nu_T|_{E_1}$. Then

$$\begin{aligned}
 & \pm \int_{E_j} \nabla_{NC}(v_C - I_{IB} v_C) \cdot D^2 u_{IB} \nu_T ds \\
 & = \int_{E_j} \frac{\partial^2 u_{IB}}{\partial x^2} \frac{\partial(v_C - I_{IB} v_C)}{\partial x} ds + \int_{E_j} \frac{\partial^2 u_{IB}}{\partial x \partial y} \frac{\partial(v_C - I_{IB} v_C)}{\partial y} ds.
 \end{aligned}$$

Since the mixed derivative $\partial^2 u_{IB} / \partial x \partial y \in P_1(T)$ is affine on T and $\partial(v_C - I_{IB} v_C) / \partial y$ is even in ξ and odd in η , a moment’s reflection reveals that the second integral is the same for $j = 1, 3$ and, hence, there is no contribution from those terms.

By (5.4), $\partial(v_C - I_{IB} v_C) / \partial x$ is an even function along E_j . Since $\partial^2 u_{IB} / \partial x^2$ is affine in y , it holds for the L^2 projection Π_{E_j} onto $P_0(E_j)$ along E_j that

$$\int_{E_j} \frac{\partial(v_C - I_{IB} v_C)}{\partial x} \frac{\partial^2 u_{IB}}{\partial x^2} ds = \int_{E_j} \frac{\partial(v_C - I_{IB} v_C)}{\partial x} \Pi_{E_j} \frac{\partial^2 u_{IB}}{\partial x^2} ds.$$

Altogether,

$$\begin{aligned} & \sum_{j=1,3} \int_{E_j} \nabla_{NC}(v_C - I_{IB} v_C) \cdot D^2 u_{IB} \nu_T ds \\ &= \int_{E_3} \frac{\partial(v_C - I_{IB} v_C)}{\partial x} \Pi_{E_3} \frac{\partial^2 u_{IB}}{\partial x^2} ds - \int_{E_1} \frac{\partial(v_C - I_{IB} v_C)}{\partial x} \Pi_{E_1} \frac{\partial^2 u_{IB}}{\partial x^2} ds. \end{aligned}$$

Recall that $\nu = (\nu_1, \nu_2)$ denotes the outer unit normal of Ω . The sum over the set \mathcal{E}_y of edges parallel to the y -axis yields

$$\begin{aligned} & \sum_{T \in \mathcal{T}} \sum_{E \in \mathcal{E}_y \cap \mathcal{E}(T)} \int_E D^2 u_{IB} \nu_T \cdot \nabla_{NC}(v_C - I_{IB} v_C) ds \\ &= \sum_{E \in \mathcal{E}_y \cap \mathcal{E}(\Omega)} \int_E \left[\Pi_E \frac{\partial^2 u_{IB}}{\partial x^2} \right]_E \left\langle \frac{\partial(v_C - I_{IB} v_C)}{\partial x} \right\rangle_E ds \\ &+ \sum_{E \in \mathcal{E}_y \cap \mathcal{E}(\Omega)} \int_E \left\langle \Pi_E \frac{\partial^2 u_{IB}}{\partial x^2} \right\rangle_E \left[\frac{\partial(v_C - I_{IB} v_C)}{\partial x} \right]_E ds \\ &+ \sum_{E \in \mathcal{E}_y \cap \mathcal{E}(\partial\Omega)} \int_E \frac{\partial(v_C - I_{IB} v_C)}{\partial x} \Pi_E \frac{\partial^2 u_{IB}}{\partial x^2} \nu_1 ds. \end{aligned} \tag{5.5}$$

The Cauchy and trace inequalities and the approximation and stability properties of the operator I_{IB} prove for the first term

$$\sum_{E \in \mathcal{E}_y \cap \mathcal{E}(\Omega)} \int_E \left[\Pi_E \frac{\partial^2 u_{IB}}{\partial x^2} \right]_E \left\langle \frac{\partial(v_C - I_{IB} v_C)}{\partial x} \right\rangle_E ds \lesssim \mu.$$

Since the jump $[\partial v_C / \partial x]_E$ vanishes, (5.4) implies that $[\partial I_{IB} v_C / \partial x]_E$ is an even quadratic function along E that vanishes at $\text{mid}(E)$. Since the derivative

$\partial^3 I_{IB} v_C / \partial x \partial y^2$ is constant, the Taylor expansion reveals, for any $E \in \mathcal{E}_y$, that

$$\int_E \left[\frac{\partial(v_C - I_{IB} v_C)}{\partial x} \right] ds = \frac{1}{2} \int_E \left[\frac{\partial^3 I_{IB} v_C}{\partial x \partial y^2} \right] (y - \text{mid}(E))^2 ds = \frac{|E|^3}{24} \left[\frac{\partial^3 I_{IB} v_C}{\partial x \partial y^2} \right]_E.$$

The combination with the second and third term of (5.5), some summation by parts and the fact that $\partial^3 I_{IB} v_C / \partial x \partial y^2$ is constant on each rectangle T and $\Pi_{E_1} \partial^2 u_{IB} / \partial x^2 = \Pi_{E_3} \partial^2 u_{IB} / \partial x^2$ for any $T \in \mathcal{T}$ lead to

$$\begin{aligned} & \sum_{E \in \mathcal{E}_y \cap \mathcal{E}(\Omega)} \int_E \left\langle \Pi_E \frac{\partial^2 u_{IB}}{\partial x^2} \right\rangle_E \left[\frac{\partial(v_C - I_{IB} v_C)}{\partial x} \right]_E ds \\ & + \sum_{E \in \mathcal{E}_y \cap \mathcal{E}(\partial\Omega)} \int_E \Pi_E \frac{\partial^2 u_{IB}}{\partial x^2} \nu_1 \frac{\partial(v_C - I_{IB} v_C)}{\partial x} ds \\ & = \sum_{E \in \mathcal{E}_y \cap \mathcal{E}(\Omega)} \left\langle \Pi_E \frac{\partial^2 u_{IB}}{\partial x^2} \right\rangle_E \frac{|E|^3}{24} \left[\frac{\partial^3 I_{IB} v_C}{\partial x \partial y^2} \right]_E \\ & + \sum_{E \in \mathcal{E}_y \cap \mathcal{E}(\partial\Omega)} \Pi_E \frac{\partial^2 u_{IB}}{\partial x^2} \nu_1 \frac{|E|^3}{24} \frac{\partial^3 I_{IB} v_C}{\partial x \partial y^2} \\ & = - \sum_{E \in \mathcal{E}_y \cap \mathcal{E}(\Omega)} \left[\Pi_E \frac{\partial^2 u_{IB}}{\partial x^2} \right]_E \frac{|E|^3}{24} \left\langle \frac{\partial^3 I_{IB} v_C}{\partial x \partial y^2} \right\rangle_E. \end{aligned}$$

The Cauchy and trace inequalities followed by an inverse estimate prove that this can be bounded by

$$\begin{aligned} & \sum_{E \in \mathcal{E}_y \cap \mathcal{E}(\Omega)} |E|^2 \left\| \left[\frac{\partial^2 u_{IB}}{\partial x^2} \right]_E \right\|_{L^2(E)} \left\| \left\langle \frac{\partial^3 I_{IB} v_C}{\partial x \partial y^2} \right\rangle_E \right\|_{L^2(E)} \\ & \lesssim \sum_{T \in \mathcal{T}} \sum_{E \in \mathcal{E}(T) \cap \mathcal{E}(\Omega) \cap \mathcal{E}_y} |E|^{1/2} \left\| \left[\frac{\partial^2 u_{IB}}{\partial x^2} \right]_E \right\|_{L^2(E)} \|D_{NC}^2 I_{IB} v_C\|_{L^2(T)} \\ & \lesssim \sqrt{\sum_{E \in \mathcal{E}(\Omega)} |E|} \left\| \left[\frac{\partial^2 u_{IB}}{\partial x^2} \right] \right\|_{L^2(E)} \|D_{NC}^2 I_{IB} v_C\|_{L^2(\Omega)}. \end{aligned}$$

The stability of the interpolation operator I_{IB} shows that this is bounded by μ . Analogous considerations for the edges parallel to the x -axis eventually prove

$$a_{NC}(u_{IB}, v_C - I_{IB} v_C) \lesssim \mu.$$

□

6 Numerical experiments

6.1 Numerical realisation

Three numerical examples investigate the reliability and efficiency of the three methods on isotropic meshes and on anisotropic tensor product meshes. Given $\beta \geq 1$ and an integer $N \geq 1$, the graded partition is determined by the points $(j/N)^\beta$ for $j = 0, \dots, N$, in the unit interval. A tensor product leads to a graded mesh on the square $(0, 1)^2$ with grading towards $(0, 0)$. The combination of such graded square domains leads to a graded mesh of the L-shaped domain with grading towards the re-entering corner (see Fig. 5).

6.2 Analytic solution

Let $u = -(x^4 - 2x^2 + 1)(y^4 - 2y^2 + 1)$ be the solution with respect to the right-hand side $f := \Delta^2 u$ on the unit square. Figure 6 shows the convergence history of the estimator from (1.1) and the exact error or in the energy norm. One observes the same convergence rates of the error and the a posteriori error estimator, which indicates reliability and efficiency in agreement with Theorems 4 and 5. This numerical experiment suggests the conjecture that the a posteriori error estimator for the Adini FEM is reliable. In particular one can observe the quadratic convergence of the Adini FEM in terms of the mesh-size for smooth solutions and equal rectangles, cf. [22].

6.3 L-shaped domain

Let $\Omega = (-1, 1)^2 \setminus ([0, 1] \times [-1, 0])$ be the L-shaped domain with constant load $f \equiv 1$. Figure 7 displays the convergence history of the estimator for uniform and graded tensor product meshes with different grading parameters $\beta = 1, 3/2, 2$. The convergence rates are improved to $1/2$. However, the grading $\beta > 1$ leads to anisotropic domains, while the constants in our error analysis depend on the aspect ratio.

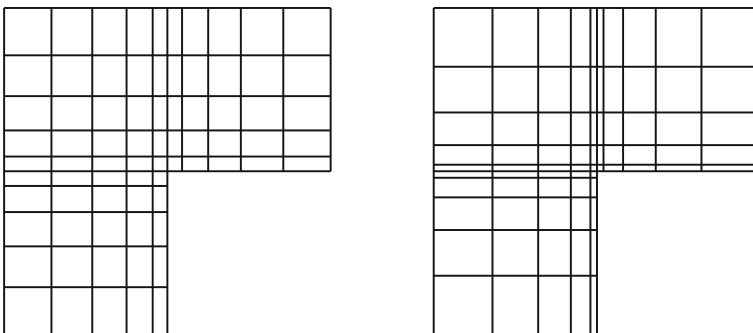


Fig. 5 Graded tensor-product meshes on the L-shaped domain

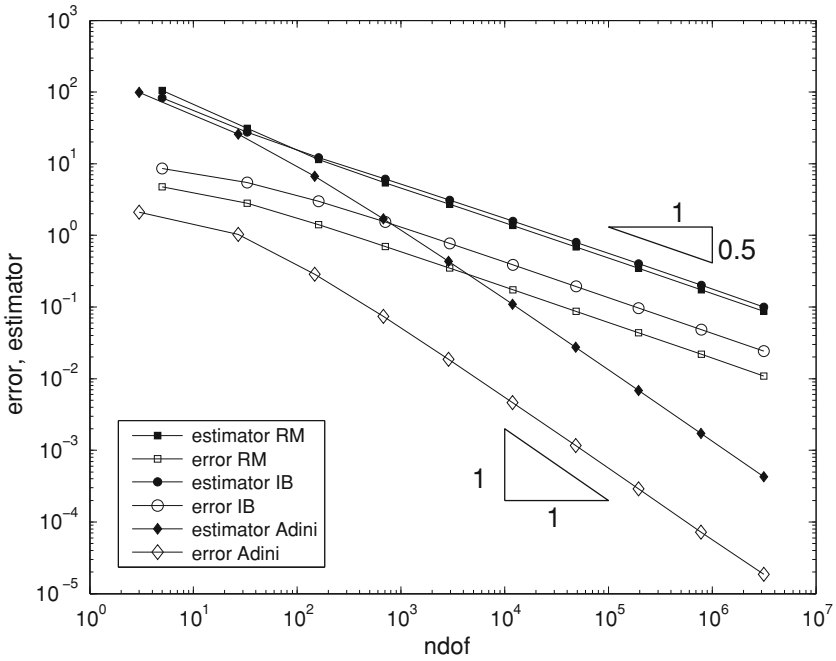


Fig. 6 Convergence history in Sect. 6.2

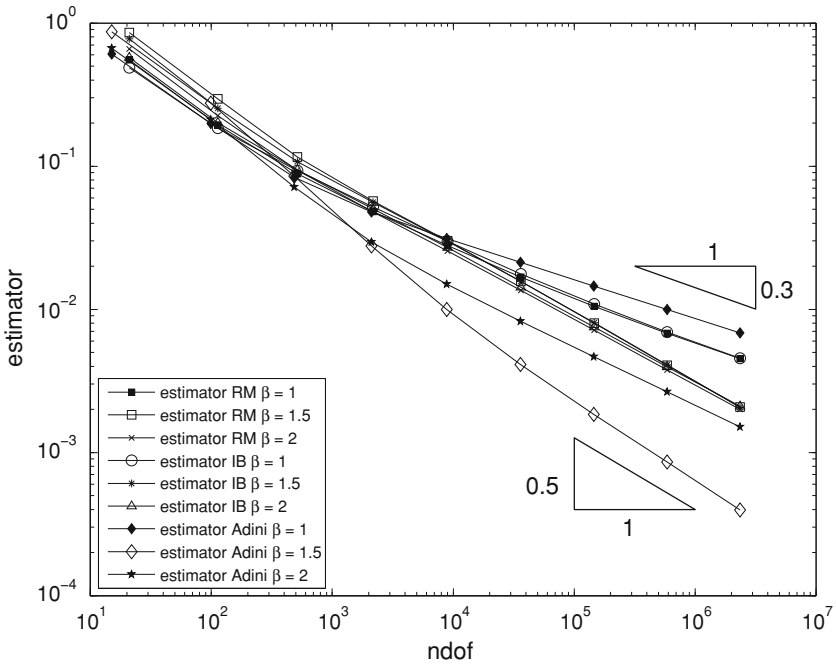


Fig. 7 Convergence history of the estimator for the L-shaped domain for uniform and graded meshes

6.4 L-shaped domain with known exact solution

Consider the L-shaped domain of Sect. 6.3 with $\omega := 3\pi/2$ and $\alpha := 0.5444837$ as a noncharacteristic root of $\sin^2(\alpha\omega) = \alpha^2 \sin^2(\omega)$. The exact singular solution from [15, p. 107], [16] reads in polar coordinates

$$u(r, \theta) = (r^2 \cos^2 \theta - 1)^2 (r^2 \sin^2 \theta - 1)^2 r^{1+\alpha} g(\theta)$$

for

$$g(\theta) = \left(\frac{1}{\alpha - 1} \sin((\alpha - 1)\omega) - \frac{1}{\alpha + 1} \sin((\alpha + 1)\omega) \right) (\cos((\alpha - 1)\theta) - \cos((\alpha + 1)\theta)) - \left(\frac{1}{\alpha - 1} \sin((\alpha - 1)\theta) - \frac{1}{\alpha + 1} \sin((\alpha + 1)\theta) \right) (\cos((\alpha - 1)\omega) - \cos((\alpha + 1)\omega)).$$

Figures 8, 9 show the convergence history of the estimator and the exact error for uniform and graded tensor-product meshes. While the convergence rate for uniform mesh refinement in Fig. 8 is sub-optimal, the solutions on the graded meshes converge with the optimal convergence rate (Fig. 9).

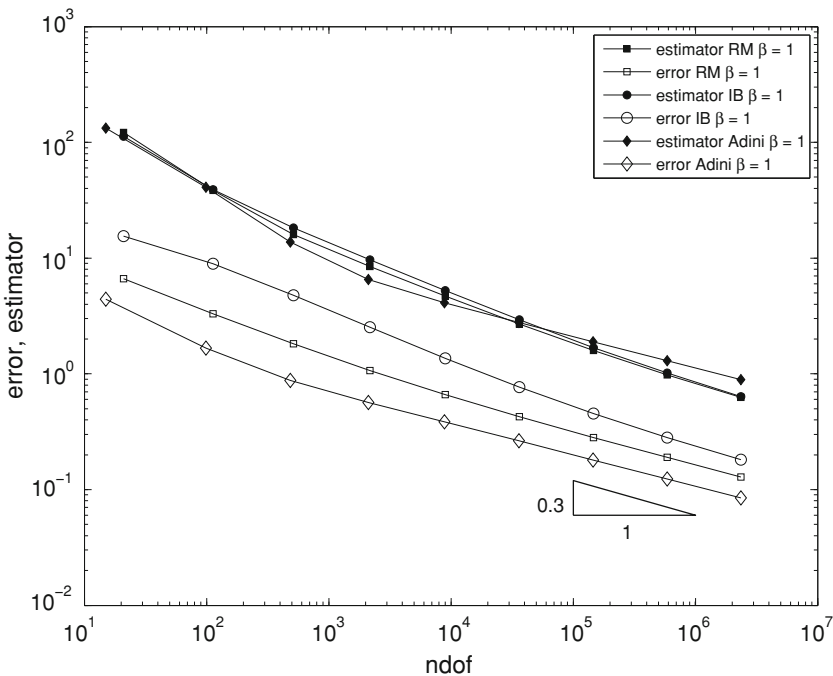


Fig. 8 Convergence history of the error and estimator for Grisvard’s example of Sect. 6.4

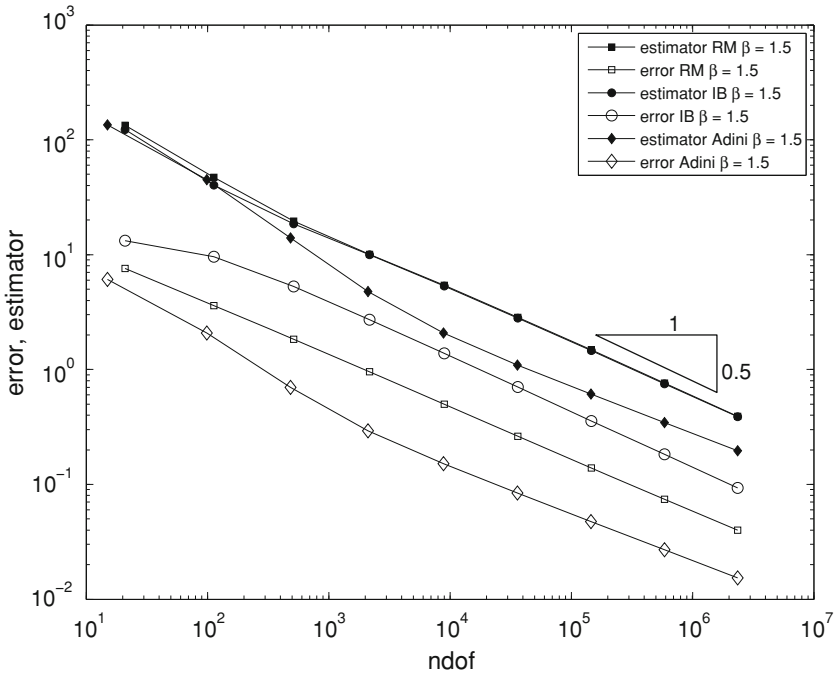


Fig. 9 Convergence history of the error and estimator for Grisvard’s example for grading parameter $\beta = 1.5$

6.5 Conclusions

- (i) All three methods develop some very small pre-asymptotic range in the sense that the graphs of error and estimator are parallel right from the beginning.
- (ii) It is conjectured that the error estimator is also reliable for the Adini finite element. The authors were not able to prove that because of the difficulties mentioned in the introduction even with the methods of Sects. 5.1 and 5.2.
- (iii) Although there is no theoretical justification, the explicit residual-based error estimator yields a reliable and efficient error bound in the examples for the Adini FEM, which supports the conjecture that the residual-based error estimator is reliable.
- (iv) Anisotropic mesh refinement on graded tensor product meshes compensates the corner singularity in the sense that the convergence rate is optimal. The overall reliability-efficiency behaviour is comparable to the isotropic case. All three methods show surprising robustness with respect to the aspect ratio.

References

1. Bartels, S., Carstensen, C.: Each averaging technique yields reliable a posteriori error control in FEM on unstructured grids I and II. *Math. Comp.* **71**(945–969), 971–994 (2002)
2. Beirao da Veiga, L., Niiranen, J., Stenberg, R.: A posteriori error estimates for the Morley plate bending element. *Numer. Math.* **106**, 165–179 (2007)

3. Beirão da Veiga, L., Niiranen, J., Stenberg, R.: A posteriori error analysis for the Morley plate element with general boundary conditions. *Int. J. Numer. Methods Eng.* **83**, 1–26 (2010)
4. Brenner, S.C.: A two-level additive Schwarz preconditioner for nonconforming plate elements. *Numer. Math.* **72**(4), 419–447 (1996)
5. Brenner, S.C., Scott, L.R.: *The mathematical theory of finite element methods*. Berlin, New York (2008)
6. Brenner, S.C., Gudi, T., Sung, L.Y.: An a posteriori error estimator for a quadratic C^0 interior penalty method for the biharmonic problem. *IMA J. Numer. Anal.* **30**, 777–798 (2010)
7. Carstensen, C.: A unifying theory of a posteriori finite element error control. *Numer. Math.* **100**, 617–637 (2005)
8. Carstensen, C., Gedicke, J., Rim, D.: Explicit error estimates for Courant, Crouzeix-Raviart and Raviart-Thomas finite element methods. *J. Comput. Math.* **30**(4), 337–353 (2012)
9. Carstensen, C., Hu, J.: A unifying theory of a posteriori error control for nonconforming finite element methods. *Numer. Math.* **107**, 473–502 (2007)
10. Carstensen, C., Hu, J., Orlando, A.: Framework for the a posteriori error analysis of nonconforming finite elements. *SIAM J. Numer. Anal.* **45**, 62–82 (2007)
11. Charbonneau, A., Dossou, K., Pierre, R.: A residual-based a posteriori error estimator for the Ciarlet-Raviart formulation of the first biharmonic problem. *Numer. Methods Partial Differ. Equ.* **13**, 93–111 (1997)
12. Ciarlet, P.G.: *The finite element method for elliptic problems*, North-Holland (1978); reprinted as *SIAM Classics in Applied Mathematics* (2002)
13. Clément, P.: Approximation by finite element functions using local regularization. *RAIRO Anal. Numér.* **9**, 77–84 (1975)
14. Georgoulis, E.H., Houston, P., Virtanen, J.: An a posteriori error indicator for discontinuous Galerkin approximations of fourth-order elliptic problems. *IMA J. Numer. Anal.* **31**, 281–298 (2011)
15. Grisvard, P.: Singularities in boundary value problems, *Recherches en Mathématiques Appliquées [Research in Applied Mathematics]* 22 (1992)
16. Gudi, T.: Residual-based a posteriori error estimator for the mixed finite element approximation of the biharmonic equation. *Numer. Methods Partial Differ. Equ.* **27**, 315–328 (2011)
17. Hansbo, P., Larson, M.G.: A posteriori error estimates for continuous/discontinuous Galerkin approximations of the Kirchhoff-Love plate. <http://www.math.chalmers.se/Math/Research/Preprints/2008/10.pdf> (2008)
18. Hu, J., Huang, Y.Q., Zhang, S.Y.: The lowest order differentiable finite element on rectangular grids. *SIAM J. Numer. Anal.* **49**, 1350–1368 (2011)
19. Hu, J., Shi, Z.C.: A new a posteriori error estimate for the Morley element. *Numer. Math.* **112**, 25–40 (2009)
20. Hu, J., Shi, Z.C., Xu, J.C.: Convergence and optimality of the adaptive Morley element method, *Numer. Math.*, 121, pp. 731–752 (2012). (See J. Hu, Z. C. Shi, J. C. Xu, Convergence and optimality of the adaptive Morley element method, Research Report 19(2009), School of Mathematical Sciences and Institute of Mathematics, Peking University, Also available online from May 2009. <http://www.math.pku.edu.cn:8000/var/preprint/7280.pdf>)
21. Huang, J.G., Huang, X.H., Xu, Y.F.: Convergence of an adaptive mixed finite element method for Kirchhoff plate bending problems. *SIAM J. Numer. Anal.* **49**, 574–607 (2011)
22. Lascaux, P., Lesaint, P.: Some nonconforming finite elements for the plate bending problem. *RAIRO Anal. Numer.* **1**, 9–53 (1985)
23. Morley, L.S.D.: The triangular equilibrium element in the solutions of plate bending problem. *Aero. Quart.* **19**, 149–169 (1968)
24. Shi, Z.C.: On the convergence of the incomplete biquadratic nonconforming plate element. *Math. Numer. Sinica* **8**, 53–62 (1986)
25. Shi, Z.C., Wang, M.: *The finite element method*. Science Press, Beijing (2010)
26. Verfürth, R.: *A review of a posteriori error estimation and adaptive mesh-refinement techniques*. Wiley-Teubner, New York (1996)
27. Wang, M., Zhang, S.: Local a priori and a posteriori error estimates of finite elements for biharmonic equation, research report 13. Peking University, School of Mathematical Sciences and Institute of Mathematics, Beijing (2006)
28. Wang, M., Xu, J.C.: The Morley element for fourth order elliptic equations in any dimensions. *Numer. Math.* **103**, 155–169 (2006)

29. Wang, M., Xu, J.C.: Some tetrahedron nonconforming elements for fourth order elliptic equations. *Math. Comp.* **76**, 1–18 (2007)
30. Wang, M., Shi, Z.C., Xu, J.C.: Some n-rectangle nonconforming elements for fourth order elliptic equations. *J. Comp. Math.* **25**, 408–420 (2007)
31. Wu, M.Q.: The incomplete biquadratic nonconforming plate element. *J. Suzhou Univ.* **1**, 20–29 (1983)